

# Generalized Relativistic Effective Core Potentials for Lanthanides

Nikolai S. Mosyagin\*

*National Research Centre "Kurchatov Institute"  
B.P.Konstantinov Petersburg Nuclear Physics Institute,  
Gatchina, Leningrad district 188300, RUSSIA*

(Received 15 November, 2016)

Generalized Relativistic Effective Core Potentials (GRECPs) for lanthanides have been constructed where the 28 innercore  $1s^2 2s^2 2p^6 3s^2 3p^6 3d^{10}$  electrons were excluded from the following GRECP calculations. Incorporation of Breit interactions in the GRECP operator is illustrated on the example of the Sm atom. Atomic test calculations have demonstrated that the generated GRECPs allow one to carry out reliable calculations at the level of "chemical accuracy" (about 1 kcal/mol or  $350 \text{ cm}^{-1}$  for transition energies). A review of the calculations on lanthanide compounds with the present and earlier generated GRECPs is given.

**PACS numbers:** 31.15.-p, 31.30.J-, 31.15.aj, 31.15.V-

**Keywords:** relativistic effective core potentials, relativistic pseudopotentials, calculations of electronic structure and properties of lanthanide compounds, accounting for Breit interactions, relativistic effects

## 1. Introduction

For lanthanide elements of Mendeleev's Periodic Table, the  $f$  shell starts first to be filled that results in some special features. Similar to actinides, lanthanides have the partially occupied  $f$  shell located in the core region shielded by the outer  $s$  and  $p$  shells. Since lanthanides in rough approximation differ from each other by the  $X$  occupation number of the core  $4f$  shell rather than that of the valence  $6s$ ,  $6p$  (and subvalence  $5d$ ) shells, they have similar physico-chemical properties, e.g., primarily the +3 oxidation state due to the presence of the ground or low-lying excited  $6s^2 5d^1$  valence configuration (in addition to the [...  $4s^2 4p^6 4d^{10} 4f^X 5s^2 5p^6$ ] core part) in all the lanthanide atoms. As a consequence of the shielding from the atom's environment, the partially occupied  $f$  shell also persists in their compounds that leads to characteristic paramagnetic and luminescent properties [14, 107], whereas the small variations in properties between different lanthanides

give fascinating possibility to select desirable parameters. In contrast to the actinides, most of the lanthanides (except promethium) have stable isotopes thus radioactive decay and emissions will not hamper their use in various fields of technology and science. Accurate calculations on lanthanide compounds are of great interest for experiments on search for space parity and time reversal nonconservation effects (e.g., on the YbF molecule [40, 41, 90, 91] or the GdGaO, GdFeO [50] and  $\text{Eu}_{0.5}\text{Ba}_{0.5}\text{TiO}_3$  crystals [88]), search for temporal variation of the fine structure constant (e.g., on the YbF, LuO, and LuS molecules [27]), the development of a new generation of frequency and time standards based on atomic optical transitions (e.g., on the Yb atoms in the optical lattice [6, 7, 39, 89]), etc. Accurate Relativistic Effective Core Potentials (RECPs) are demanded to carry out the required calculations by an economic manner.

Breit effects (which are the two-electron relativistic corrections to conventional Coulomb interactions between electrons) for low atomic excitation energies are largest for both the actinides and lanthanides. Breit contribution can attain several kcal/mol for energies of the

---

\*E-mail: mosyagin\_ns@pnpi.nrcki.ru; URL: <http://qchem.pnpi.spb.ru>

transitions between low-lying atomic states with different valence  $f$  shell occupation numbers. These contributions can be sometimes comparable with the corresponding transition energies calculated without accounting for Breit interactions (see the errors in the 5th column of Table 1). Thus, lanthanides seem to be suitable for studying the influence of Breit effects on chemistry. It should be noted that the available RECPs for lanthanides were generated more than 20 years ago by other groups [18, 20, 81] without accounting for Breit interactions.

The lanthanide compounds are rather difficult objects for accurate quantum chemical calculations. Computational difficulties are caused by significant relativistic effects, high density of low-lying electronic states, and complexity of electronic structure of lanthanides that cause high demands on both the computing resources and effectiveness of computational methods as well as computer codes. The relativistic effects are sometimes neglected in calculations on light element compounds. However, these effects are rapidly increased with the nuclear charge  $Z$  and they may amount up to 100 kcal/mol for energies of the transitions between low-lying atomic states of lanthanides (see the errors in the last column of Table 1) thus the relativistic effects should be taken into account in accurate calculations. The difference between the one-electron energies of the valence  $6s_{1/2}$  spinors and the  $4f_{5/2}$ ,  $4f_{7/2}$  ones for lanthanides is not too high as one can see from Table 2. (Below for brevity, the  $nl_{j=|l-1/2|}$  and  $nl_{j=|l+1/2|}$  pair will be sometimes designated as just  $nl$ , where  $n$ ,  $l$ , and  $j$  are the principal, orbital and total quantum numbers. The  $nl$ ,  $nl'$ , and  $nl''$  sets will be further designated by the  $nl'l''$  indices, etc.) Therefore, the energies of excitations from (and into) the  $4f$  shell are rather low. This leads to appearance of the states with different occupation numbers of the  $4f$  shell among the ground and low-lying excited states for the lanthanide atoms and low charged ions. The large number of low-lying states results in strong static correlation effects between the

states of the same symmetry which have to be taken into account in accurate calculations. Most of lanthanides have open  $4f$  shells in the ground states of their atoms and low charged ions. Therefore, the  $4f$  spinors should be considered as valence ones, accounting also for their small one-electron energies. However, the  $4f$  shells are localized in the same spatial region as the  $4spd$  and  $5sp$  shells (see the average radii in Table 2), which have relatively large negative one-electron energies and should be considered as core-like states, whereas the  $6sp$  shells are valence. Thus, the  $4f$  shell has the twofold (core and valence) features. Low-energy excitations from the  $4f$  shell will lead to its non-negligible relaxation and will also affect the outercore  $4spd$  and  $5sp$  shells. Similar to actinides and in contrast to the main group elements, the core  $(n-2)sp$  and  $(n-1)sp$  shells can not be “frozen” in accurate calculations to reduce the computational efforts (the valence shells are denoted  $nsp$  where  $n = 6$  for lanthanides).

There are several options to perform lanthanide compound calculations. The straightforward way is to use Dirac-Coulomb (DC) or Dirac-Coulomb-Breit (DCB) Hamiltonians [33, 49, 58, 80, 84]. The latter is nominally the most accurate of known relativistic Hamiltonians. In particular, a series of four-component all-electron calculations with the DC Hamiltonian on the YbF molecule was carried out by different authors [2, 11, 28, 68–73, 76, 79, 85]. Their results are compared with that of the corresponding RECP and semiempirical calculations in Table 3 and Subsection 5.2. The computational efforts in quantum chemical calculations employing basis set expansions of one-electron spinors very rapidly increase with the number of basis functions. The application of four-component Dirac spinors requires the use of significantly larger primitive (usually Gaussians) basis sets (to describe properly their small components) as compared to the one- and two-component quasirelativistic approaches. Such calculations exploiting Douglas-Kroll-Hess Hamiltonian [22, 38] are reported for the LiYb

molecule [32, 109]. Still, too large set of primitive basis functions is required to describe accurately the large number of the radial oscillations, which valence spinors have in the all-electron calculation due to their orthogonality to the core spinors.

The RECP or pseudopotential method is widely used in calculations on molecules containing heavy atoms [26, 87] because it reduces drastically the computational cost at the integral generation, self-consistent field (SCF) calculation and integral transformation stages. Different RECP versions are available for lanthanides in the literature [18, 20, 81]. They have been applied in practical calculations [13, 15, 17, 19, 51, 52, 100, 104]. It was shown in papers [66, 94, 101] that the conventional radially-local (semi-local) form of the RECP operator (used by many groups up to now but proposed and first applied 50 years ago by Abarenkov and Heine [1, 37] to nonrelativistic calculations of solids) is limited in accuracy and some non-local corrections to the RECP operator were suggested [93–95, 101] which have already allowed one to improve significantly the RECP accuracy [42, 59, 66, 94]. The new generation of the RECPs is able to provide the accuracy as that attainable in the most advanced four-component approaches at many times smaller computational cost. Accordingly, it is possible to use modeling techniques for essentially more complex lanthanide compounds. The generalized RECPs (GRECPs) have been generated for all the lanthanides to perform calculations of electronic structure and properties of their compounds economically but with very high accuracy. Accuracy of these GRECPs is analyzed in atomic calculations. A review of the calculations on lanthanide compounds with the present and earlier generated GRECPs is given.

## 2. The Scheme of the GRECP Generation

The GRECP generation technique [62, 66, 77, 101] is based on the RECP construction

scheme proposed in Refs. [16, 25, 31, 36, 53, 75]. The principal distinctive features of the GRECP technique are (a) generation of the GRECP components for both the valence and outercore electrons with different  $n$  but with the same  $lj$  pair and (b) addition of non-local (separable) terms to the conventional semi-local RECP operator. Below, these GRECP components will be also called the potentials. There are also some modifications [64, 66, 94] in respect to the spinor smoothing procedure [16] and the procedure of Gaussian approximation of the numerical potentials [56, 75]. The main steps of the GRECP generation scheme are:

1. The numerical all-electron relativistic calculation of a generator state is carried out for an atom under consideration. For this purpose, we use the modern Dirac-Fock-Breit (DFB) version of the atomic Dirac-Fock (DF) code [12]. Fermi nuclear charge distribution is used in the all-electron calculations in the present paper (unless otherwise explicitly stated). As a result, the radial parts of the large  $\frac{1}{r}P_{nlj}(r)$  and small  $\frac{1}{r}Q_{nlj}(r)$  components of the four-component DFB spinors and their  $\varepsilon_{nlj}$  one-electron energies are obtained. In the present version of the lanthanide GRECPs, the spinors with  $n \leq 3$  will be excluded from the GRECP calculations as innercore ones (i.e. the 28 electron core), the  $4spd$ ,  $5sp$  and  $6sp$ ,  $5d$ ,  $4f$  ones will be considered as the outercore and valence ones, respectively.
2. The radial parts of the numerical pseudospinors  $\frac{1}{r}\tilde{\varphi}_{nlj}(r)$  are constructed of that of the large components of both the valence and outercore DFB spinors so that the innermost pseudospinors for each  $lj$  pair have no radial nodes (nodeless), the next pseudospinors have one radial node, and so forth. (Further, the node will mean the radial node.) These pseudospinors

satisfy the following conditions:

$$\begin{aligned} \tilde{\varphi}_{nlj}(r) &= \begin{cases} P_{nlj}(r), & r \geq R_c, \\ f(r), & r < R_c, \end{cases} \\ f(r) &= r^\gamma \sum_{i=0}^5 a_i r^i, \\ l &= 0, 1, \dots, L, \quad j = |l \pm 1/2|, \\ n &= n_{c1}, n_{c2}, \dots, n_{cN}, n_v, \end{aligned} \quad (1)$$

where  $n = n_{c1}, n_{c2}, \dots, n_{cN}$  and  $n_v$  are the principal quantum numbers of outercore and valence electrons, respectively,  $L$  is one more than the highest orbital angular momentum of the innercore spinors, and  $r$  is the radial variable. The leading power  $\gamma$  in the polynomial  $f(r)$  is typically chosen to be close to  $L + 1$  in order to ensure a sufficient ejection of the valence and outercore electrons from the innercore region. The  $a_i$  coefficients are determined by the following requirements:

- $\tilde{\varphi}_{nlj}$  are normalized;
- $\tilde{\varphi}_{n_{c1}lj}, \tilde{\varphi}_{n_{c2}lj}, \dots, \tilde{\varphi}_{n_{cN}lj}$ , and  $\tilde{\varphi}_{n_vlj}$  are orthogonal with a high degree of accuracy;
- $f$  and its first four derivatives match  $P_{nlj}$  and its derivatives;
- $f$  is a smooth and nodeless function;
- $\tilde{\varphi}_{nlj}$  ensure a sufficiently smooth shape of the corresponding potential ( $U_{nlj}$ , see the next item).

$R_c$  is chosen near such an extremum of the spinor that the corresponding pseudospinor has the defined above number of nodes. In practice, the  $R_c$  radii for the different spinors should be chosen close to each other in order to generate smooth potentials. (Below, the pseudospinors will be sometimes also called the spinors.)

3. The numerical potentials  $U_{nlj}$  are derived for each  $lj$  pair for the valence and outercore pseudospinors so that the  $\tilde{\varphi}_{nlj}$

are solutions of the nonrelativistic-type Hartree-Fock (HF) equations in the  $jj$ -coupling scheme for a ‘‘pseudoatom’’ with the removed innercore spinors

$$\begin{aligned} U_{nlj}(r) &= \tilde{\varphi}_{nlj}^{-1}(r) \left[ \left( \frac{1}{2} \frac{d^2}{dr^2} - \frac{l(l+1)}{2r^2} \right. \right. \\ &+ \frac{Z^*}{r} - \tilde{J}(r) + \tilde{K}(r) + \varepsilon_{nlj} \left. \right) \tilde{\varphi}_{nlj}(r) \\ &\left. + \sum_{n' \neq n} \varepsilon_{n'nlj} \tilde{\varphi}_{n'lj}(r) \right], \end{aligned} \quad (2)$$

where  $Z^* = Z - N_{ice}$  is the effective innercore charge,  $N_{ice}$  is the number of the InnerCore Electrons,  $\tilde{J}$  and  $\tilde{K}$  are the Coulomb and exchange operators calculated with the valence and outercore pseudospinors, and  $\varepsilon_{n'nlj}$  are the off-diagonal Lagrange multipliers.

In the case of the pseudospinor with nodes, the potential is singular because the zeros of the denominator and numerator do not coincide. However, these zeros are close to each other in practice as it had been demonstrated in Ref. [92] and the most appropriate solution of this problem is the interpolation of the potential in a vicinity of the pseudospinor node. The error of reproducing the one-electron energy due to such an interpolation can be made small enough (because the pseudospinors are small in the vicinity of the node and the node position is not virtually changed at forming chemical bond and low-energy excitations). It does not exceed the errors of the GRECP approximation caused by smoothing the spinors and the approximate treatment of the interaction with the innercore electrons [101]. Then, one can write the GRECP as a Hermitian operator in the spinor representation (corresponding

to the  $jj$ -coupling scheme)

$$\begin{aligned}
& \hat{U}^{\text{GRECP}} = U_{n_v L J}(r) \\
& + \sum_{l=0}^L \sum_{j=|l-1/2|}^{l+1/2} [U_{n_v l j}(r) - U_{n_v L J}(r)] \hat{P}_{l j} \\
& + \sum_{n_c} \sum_{l=0}^L \sum_{j=|l-1/2|}^{l+1/2} \left\{ [U_{n_c l j}(r) - U_{n_v l j}(r)] \right. \\
& \quad \left. \tilde{P}_{n_c l j} + \tilde{P}_{n_c l j} [U_{n_c l j}(r) - U_{n_v l j}(r)] \right\} \\
& \quad - \sum_{n_c, n'_c} \sum_{l=0}^L \sum_{j=|l-1/2|}^{l+1/2} \tilde{P}_{n_c l j} \quad (3) \\
& \left[ \frac{U_{n_c l j}(r) + U_{n'_c l j}(r)}{2} - U_{n_v l j}(r) \right] \tilde{P}_{n'_c l j}, \\
& \hat{P}_{l j} = \sum_{m_j=-j}^j |l j m_j\rangle \langle l j m_j|, \\
& \tilde{P}_{n_c l j} = \sum_{m_j=-j}^j |\widetilde{n_c l j m_j}\rangle \langle \widetilde{n_c l j m_j}|,
\end{aligned}$$

where  $|l j m_j\rangle \langle l j m_j|$  is the projector on the two-component spin-angular eigenfunction  $\chi_{l j m_j}(\phi, \sigma)$  of the operators of the square  $j^2$  and projection  $j_z$  of the one-electron total momentum  $\hat{j}$ ,  $|\widetilde{n_c l j m_j}\rangle \langle \widetilde{n_c l j m_j}|$  is the projector on the two-component outercore pseudospinors  $\frac{1}{r} \tilde{\varphi}_{n_c l j}(r) \chi_{l j m_j}(\phi, \sigma)$  (which are functions of the radial  $r$ , angular  $\phi$ , and spin  $\sigma$  variables),  $m_j$  is the quantum number of the total momentum projection, and  $J = L + 1/2$ .

Thus, the many-electron DC(B) Hamiltonian is replaced by the effective Hamiltonian with the GRECP

$$\begin{aligned}
\hat{H}^{\text{Ef}} &= \sum_p [\hat{h}^{\text{Schr}}(\tau_p) + \hat{U}^{\text{GRECP}}(\tau_p)] \\
& + \sum_{p>p'} \frac{1}{r_{pp'}} \quad (4)
\end{aligned}$$

written only for valence and outercore electrons denoted here by composite indices

$p \equiv (n, l, j, m_j)$ , where  $\tau \equiv (r, \phi, \sigma)$  and  $r_{pp'}$  is the distance between the electrons  $p$  and  $p'$ . The GRECP operator  $\hat{U}^{\text{GRECP}}$  simulates interactions of the explicitly treated (outercore and valence) electrons with those which are excluded from the GRECP calculation. In Eq. (4),  $\hat{h}^{\text{Schr}}$  is the nonrelativistic one-electron Schrödinger operator for a point-charge Coulomb field

$$\hat{h}^{\text{Schr}} = -\frac{1}{2} \nabla^2 - \frac{Z^*}{r}, \quad (5)$$

where  $\nabla$  is the gradient operator. Contrary to the four-component (relativistic) wave function used in DC(B) calculations, the pseudo-wave function in the GRECP case can be both two- and one-component (see the next item).

4. With a view to be used in molecular calculations with Gaussian basis sets, the numerical potentials taken in the form

$$\begin{aligned}
& U_{n_v L}^{\text{AREP}}(r) r^2, \\
& [U_{n_v l}^{\text{AREP}}(r) - U_{n_v L}^{\text{AREP}}(r)] r^2 \quad (l \neq L), \\
& \quad \Delta U_{n_v l}(r) r^2 \quad (l \neq 0), \\
& [U_{n_c l j}(r) - U_{n_v l j}(r)] r^2, \quad (6)
\end{aligned}$$

where

$$\begin{aligned}
U_{n_v l}^{\text{AREP}}(r) &= \frac{l+1}{2l+1} U_{n_v l+}(r) \\
& + \frac{l}{2l+1} U_{n_v l-}(r), \quad (7)
\end{aligned}$$

$$\Delta U_{n_v l}(r) = U_{n_v l+}(r) - U_{n_v l-}(r) \quad (8)$$

for the valence electrons and  $l\pm \equiv (l, j = l \pm 1/2)$  are usually fitted by Gaussian functions. The latter functions are ordinarily written as

$$\sum_i c_i r^{k_i} \exp(-\alpha_i r^2), \quad (9)$$

where  $\alpha_i > 0$  and  $c_i$  are real parameters,  $k_i$  is equal to 0, 1, or 2. The numerical

pseudospinors are fitted by Gaussians in the form

$$\tilde{\varphi}_{nlj}(r) = r^{l+1} \sum_i c_i M_i \exp(-\alpha_i r^2), \quad (10)$$

where  $M_i$  are the standard normalization factors.

For application of the GRECP to molecular calculations with the spin-orbital basis sets which are used in most existing quantum-chemical codes, the GRECP operator (3) should be transformed to the spin-orbital representation (which corresponds to the  $LS$ -coupling scheme) following work [36]. The components of the spin-averaged part of the GRECP operator are called the averaged relativistic effective potentials (AREP) and are written in form (7) for the valence electrons and

$$\begin{aligned} \hat{U}_{ncl}^{\text{AREP}}(r) &= \frac{l+1}{2l+1} \hat{V}_{ncnvl+}(r) \\ &+ \frac{l}{2l+1} \hat{V}_{ncnvl-}(r), \quad (11) \end{aligned}$$

$$\begin{aligned} \hat{V}_{ncnvlj}(r) &= [U_{nclj}(r) - U_{nvlj}(r)] \tilde{P}_{nclj}(r) \\ &+ \tilde{P}_{nclj}(r) [U_{nclj}(r) - U_{nvlj}(r)] \\ &- \sum_{n'_c} \tilde{P}_{nclj}(r) \left[ \frac{U_{nclj}(r) + U_{n'_clj}(r)}{2} \right. \\ &\quad \left. - U_{nvlj}(r) \right] \tilde{P}_{n'_clj}(r) \end{aligned}$$

for the outercore electrons, where  $\tilde{P}_{nclj}(r)$  is the radial projector on the outercore pseudospinors  $\frac{1}{r} \tilde{\varphi}_{nclj}(r)$ . Obviously, these components may be used instead of the nonrelativistic generalized ECP components in the above-mentioned codes in order to take into account the scalar relativistic effects.

The operator of the effective spin-orbit interaction can also be derived following paper [36]. Its components are called the

effective spin-orbit potentials (ESOP) and can be written as (see also Eq. (8))

$$\Delta \hat{U}_{ncl}(r) = \hat{V}_{ncnvl+}(r) - \hat{V}_{ncnvl-}(r),$$

$$\hat{U}_{nl}^{\text{ESOP}} = \frac{2\Delta \hat{U}_{nl}(r)}{2l+1} \hat{P}_l \hat{l} \hat{s}, \quad (12)$$

$$\hat{P}_l = \sum_{m_l=-l}^l |lm_l\rangle \langle lm_l|,$$

where  $|lm_l\rangle \langle lm_l|$  is the angular projector on the spherical function  $Y_{lm_l}(\phi)$ ,  $m_l$  is the quantum number of the orbital momentum projection,  $\hat{l}$  and  $\hat{s}$  are the operators of orbital and spin momenta.

Neglecting the difference between  $U_{n_vL}^{\text{AREP}}$  and  $U_{n_vLJ}$  for virtual pseudospinors with  $l > L$ , the GRECP operator (3) is rewritten in the form

$$\begin{aligned} \hat{U}^{\text{GRECP}} &\simeq U_{n_vL}^{\text{AREP}}(r) \\ &+ \sum_{l=0}^{L-1} [U_{n_vl}^{\text{AREP}}(r) - U_{n_vL}^{\text{AREP}}(r)] \hat{P}_l \\ &+ \sum_{n_c} \sum_{l=0}^L \hat{U}_{ncl}^{\text{AREP}}(r) \hat{P}_l \\ &+ \sum_{l=1}^L [\hat{U}_{n_vl}^{\text{ESOP}} + \sum_{n_c} \hat{U}_{ncl}^{\text{ESOP}}] \hat{P}_l, \quad (13) \end{aligned}$$

where the following identities for the  $\hat{P}_{lj}$  projectors were used:

$$\begin{aligned} \hat{P}_{l\pm}(\phi, \sigma) &= \frac{1}{2l+1} \left[ \left( l + \frac{1}{2} \pm \frac{1}{2} \right) \hat{P}_l(\phi) \right. \\ &\quad \left. \pm 2\hat{P}_l(\phi) \hat{l} \hat{s} \hat{P}_l(\phi) \right]. \quad (14) \end{aligned}$$

### 3. Accounting for Breit Contributions with the help of GRECP

The contributions of Breit interaction between electrons from different shells (denoted

below  $\mathcal{B}_{pp'}$ ) to the total energy of a heavy atom were analyzed in details in papers [62, 77]. Using the state averaged over the nonrelativistic  $4f^66s^2$  configuration of the Sm atom as an example, we have derived these contributions from the numerical DFB calculation where the  $4f$  and  $6s$  spinors were grouped together as the valence ones ( $p \equiv v$ ), whereas the  $4spd$ ,  $5sp$  ones were considered as the outercore spinors ( $p \equiv c$ ), and the  $1s$ ,  $2sp$ ,  $3spd$  ones were the innercore spinors ( $p \equiv f$ ). The largest contributions for the interactions between electrons from these groups are

$$\begin{aligned} \max[\mathcal{B}_{ff'}] &= \mathcal{B}_{1s1/2,1s1/2} = 723\,012 \text{ cm}^{-1}, \\ \max[\mathcal{B}_{fc}] &= \mathcal{B}_{1s1/2,4p1/2} = 2\,566 \text{ cm}^{-1}, \\ \max[\mathcal{B}_{cc'}] &= \mathcal{B}_{4p1/2,4p1/2} = 98 \text{ cm}^{-1}, \\ \max[\mathcal{B}_{fv}] &= \mathcal{B}_{3d3/2,4f5/2} = 79 \text{ cm}^{-1}, \\ \max[\mathcal{B}_{vv'}] &= \mathcal{B}_{4f5/2,4f5/2} = 31 \text{ cm}^{-1}, \\ \max[\mathcal{B}_{cv}] &= \mathcal{B}_{4d3/2,4f5/2} = 27 \text{ cm}^{-1}. \end{aligned}$$

Let us consider approximations in accounting for Breit interaction, that we made when outercore and valence electrons are included in GRECP calculations with Coulomb two-electron interactions, but innercore electrons are absorbed into the GRECP. Though  $\mathcal{B}_{ff'}$  does not contribute directly to “differential” (valence) properties such as energies of transitions between different valence configurations, it can lead to essential relaxation of both core and valence shells. This relaxation is taken into account when Breit interaction is treated by self-consistent way in the framework of the DFB method [54, 78].

The innercore electrons occupy closed shells. The contributions from  $\mathcal{B}_{fv}$  and especially  $\mathcal{B}_{fc}$ , are quite essential for calculation at the level of “chemical accuracy” (about 1 kcal/mol or  $350 \text{ cm}^{-1}$  for transition energies). This accuracy level is, in general, determined by the possibilities of modern correlation methods and computers already for compounds of light elements. The innercore electrons can be considered as “frozen” in most physical-chemical processes of interest. Therefore, the effective operators for  $\mathcal{B}_{fv}$  and  $\mathcal{B}_{fc}$  acting on the valence and outercore shells,  $\hat{B}_{fv}^{\text{Ef}}$  and  $\hat{B}_{fc}^{\text{Ef}}$ , are of the same kind as the exchange

$f-v$  and  $f-c$  contributions of the SCF field in the Huzinaga-type potential [10, 83], i.e. these terms can be well approximated by the spin-dependent potential of the form:

$$\begin{aligned} \hat{B}_{fv}^{\text{Ef}} + \hat{B}_{fc}^{\text{Ef}} &= \sum_{lj} U_{nvlj}^{\text{Br}}(r) \hat{P}_{lj} \\ &+ \sum_{nclj} [U_{nclj}^{\text{Br}}(r) - U_{nvlj}^{\text{Br}}(r)] \tilde{P}_{nclj}, \end{aligned}$$

which has basically the same spin-angular structure as the GRECP has. Thus, it can be taken into account directly when the DFB (not DF) calculation [33] is performed to generate outercore and valence four-component spinors and their one-electron energies (see Item 1 in Section 2) but the conventional interelectronic Coulomb interaction is used instead of the Coulomb-Breit one in the procedure of inversion of the two-component HF equations for generating the GRECP components (see Item 3 in Section 2). Afterwards, one have to consider only the Coulomb interaction between the explicitly treated electrons in the following GRECP calculations.

Due to small relaxation of outercore shells in most processes of interest, these shells can be also considered as “frozen” when analyzing Breit contributions and the  $\mathcal{B}_{cc'}$  and  $\mathcal{B}_{cv}$  terms can be taken into account similarly to the  $\mathcal{B}_{fc}$  and  $\mathcal{B}_{fv}$  ones. The error of this approximation will be additionally suppressed by relative weakness of Breit interaction with the outercore electrons as compared to the innercore ones.

The  $\mathcal{B}_{cv}$  and  $\mathcal{B}_{vv'}$  contributions are negligible for the “chemical accuracy” of calculation. Strictly speaking, we do not neglect Breit interaction between valence electrons completely in the GRECP calculations. It would be so, if we did not take into account Breit interaction between valence electrons at the stage of the DFB calculations as well. But it is even more convenient and natural to account for Breit interaction between the valence electrons at this stage. In the latter case, the changes in one-electron energies and shapes of the spinors (not only valence) of the generator state due to this

interaction will be taken into account. However, the corresponding changes for other states are not the same as for the generator state. So, we can say that in some sense we “freeze” Breit interaction between the valence electrons from the generator state.

Therefore, the above considerations provide us a good background for approximating two-electron Breit interaction by an one-electron GRECP operator that should work well for both lanthanides and other elements at the required level of accuracy. The numerical tests of the GRECPs accounting for the Breit effects are considered in Section 4.

#### 4. Atomic Tests of GRECP Accuracy

The generated GRECPs have been tested in atomic SCF calculations which are largely sufficient to analyze the quality of different (G)RECP versions. These calculations are numerical (finite-difference) that allows one to exclude the errors due to incompleteness of the basis sets and compare the “pure” errors inherent to different GRECP versions. In the framework of the atomic SCF approach, one can easily perform the reference all-electron calculations with the DCB Hamiltonian. The errors appearing already in the atomic one-configuration GRECP studies as compared to the DFB ones are, obviously, inherent for the corresponding GRECP. These errors will be added to the errors appearing in the following correlation and molecular calculations with this GRECP. Therefore, the atomic one-configuration calculations give upper limits on the accuracy of the tested GRECP versions. The all-electron calculations were carried out employing the modern DFB version of the numerical atomic DF code [12]. The GRECP calculations were carried out with the help of the numerical atomic two-component HF code in the *jj*-coupling scheme [101]. The results of the DFB calculations are presented in the second column of Tables 1, 4, 5, and 6, whereas the errors of

their reproducing in the different all-electron and GRECP calculations are given in the following columns.

To estimate contribution from the relativistic effects, the DFB calculations with the light velocity increased in 1000 times were carried out. These calculations are excellent approximation of the nonrelativistic HF ones in the *jj*-coupling scheme (except perhaps the nuclear model). Their errors are presented in the last column of Tables 1 and 5. One can see that the relativistic effects are significant for lanthanides and should be accounted for in accurate calculations. The contribution from the finite size of the nucleus is negligible in comparison with the level of the “chemical accuracy”. The largest error due to neglecting Breit interactions is  $1600 \text{ cm}^{-1} \approx 4.5 \text{ kcal/mol}$  that is larger than the “chemical accuracy” level. One can also see that the differences between accounting for Breit interactions in the framework of the perturbation theory and by self-consistent manner are small.

As it was noted in the Introduction, the open *4f* shells in lanthanides, on the one hand, are close in one-electron energies to the valence *6sp* shells and, on the other hand, are spatially close to the outercore *5sp* and *4spd* shells. That leads to advisability to include all the electrons with the principal quantum numbers  $n \geq 4$  explicitly in GRECP calculations. Thus, the 28-electron inner cores are used in the present GRECP versions for lanthanides. The valence and core GRECP versions were derived from the original GRECP version by neglecting the differences between the outercore and valence potentials. Thus, the valence GRECP operator is a semi-local one with the *6s*, *6p*, *5d*, and *4f* components of the original GRECP version (i.e. the first and second lines in Eq. (3) or the terms containing  $U_{n_v}$  in Eq. (13)). The main difference of the valence GRECP from the conventional RECPs is that the components of the former were constructed for nodal valence pseudospinors. Thus, these are the valence potentials (not the outercore or somehow averaged ones) which act on the valence electrons

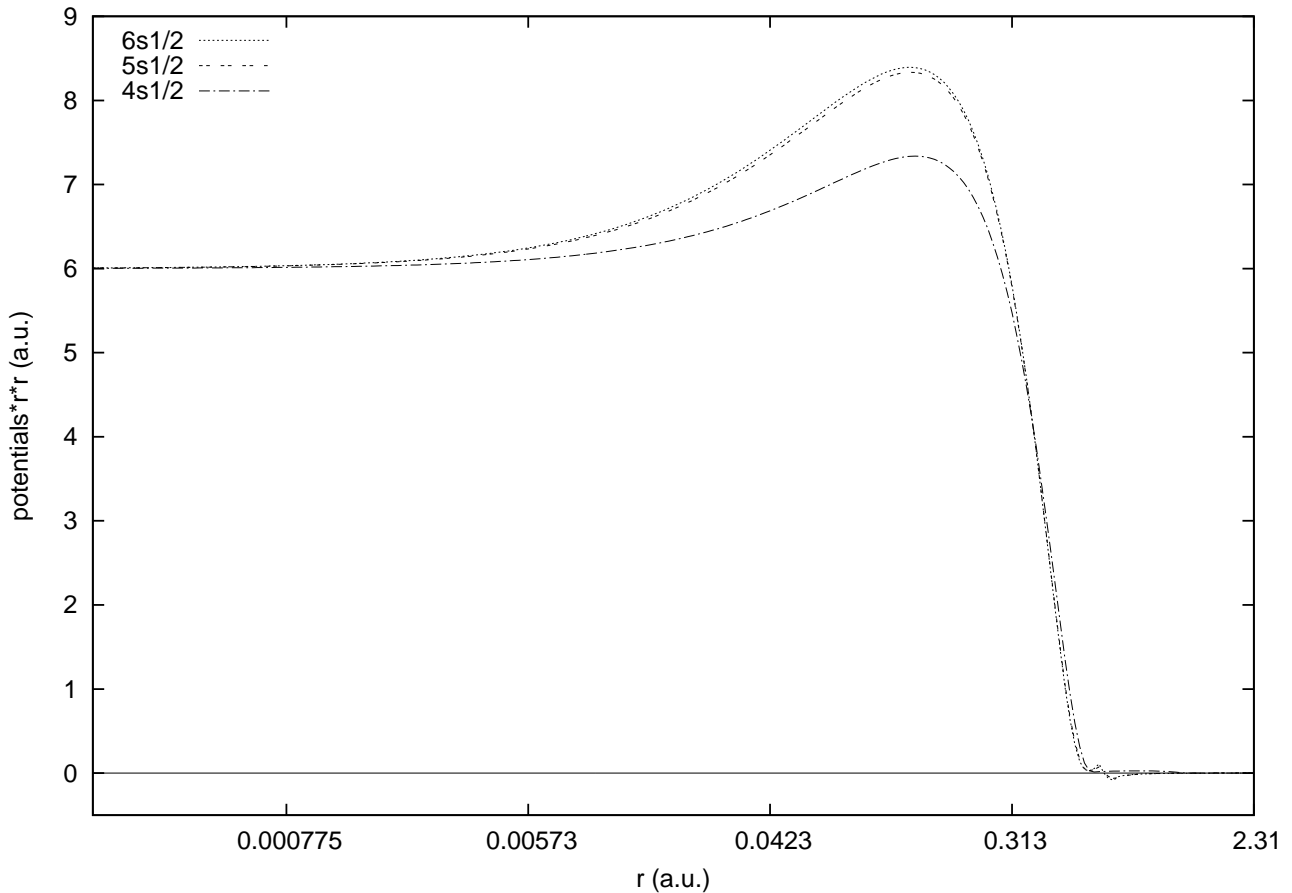


Figure 1. The GRECP components (multiplied by  $r^2$ ) for the valence ( $6s_{1/2}$ ) and outercore ( $5s_{1/2}$ ,  $4s_{1/2}$ ) subshells of samarium. Note that the logarithmic scale for  $r$  is used.

in this GRECP version (the differences in the potentials can be seen from Figure 1). Two different core GRECP operators contain the  $5spd$ ,  $4f$  and  $4spdf$  components, respectively.

The  $\langle r^2 \rangle$  matrix elements (ME) characterize the wavefunction in the outermost region. They are reproduced in the GRECP calculations with high accuracy for the case of the valence  $6sp$  pseudospinors and with good accuracy for the outercore  $4f$  and  $5d$  ones as one can see in Table 6. In contrast to actinides [67], the shapes of the large components for the  $f$  spinors are only slightly modified in the innercore region at the GRECP generation (to obtain the proper nonrelativistic behaviour at the origin and normalization), therefore both the  $\langle r^2 \rangle$

MEs for the  $f$  shell and the energies for the transitions where the  $f$  spinors are directly involved, e.g., transitions with the change of the  $f$  shell occupation number (i.e. the 4-6th transitions in Table 4), are reproduced significantly better in the case of lanthanides. One can see from Table 4 that the non-local original GRECP version allows one to carry out reliable calculations of lanthanide compounds at the level of the “chemical accuracy”. The errors in transition energies for the semi-local (valence and core) GRECP versions are essentially higher than that for the original GRECP. The errors in reproducing  $\langle r^2 \rangle$  for the  $6sp$  spinors are also essentially increased for the semi-local (valence and especially core) GRECP versions. One can also see from the comparison of

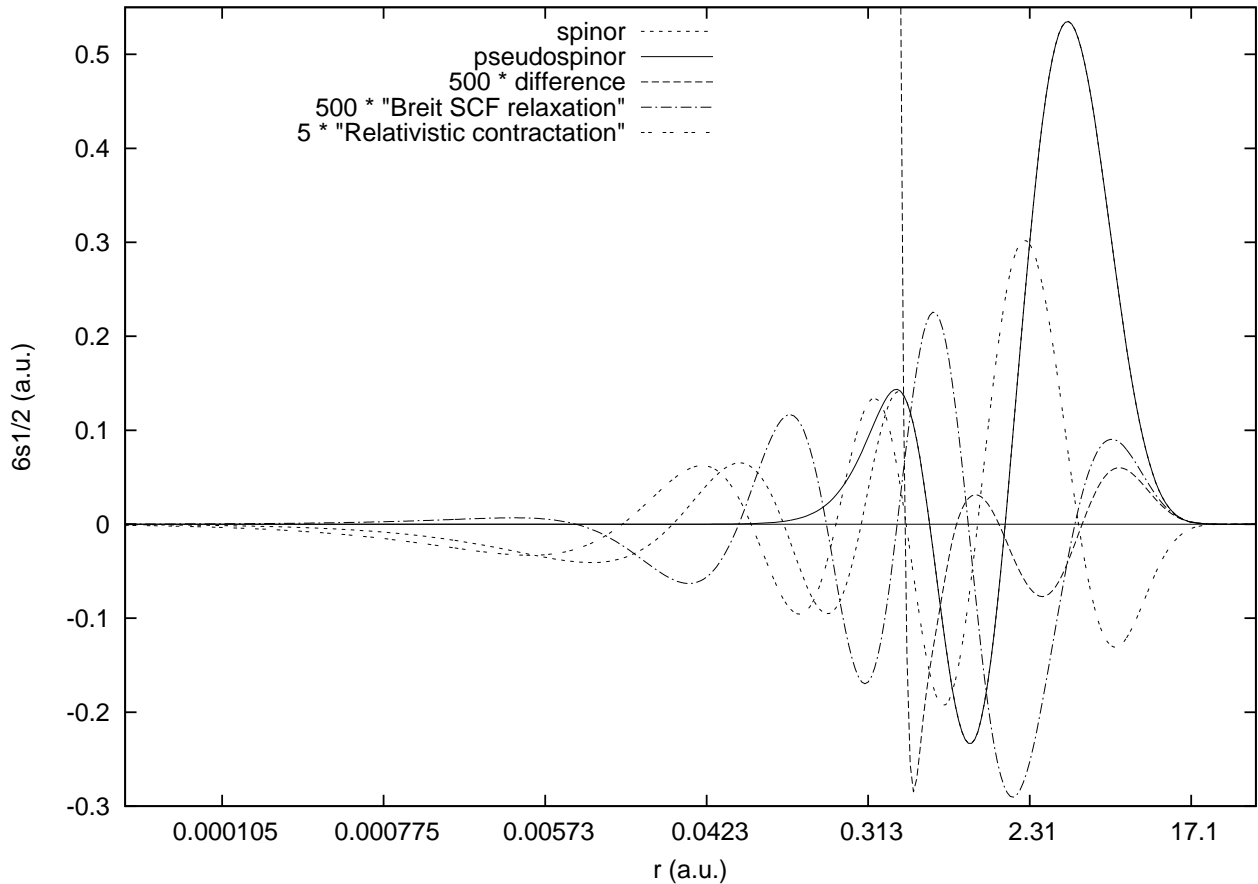


Figure 2. The  $\tilde{\varphi}_{6s1/2}(r)$  pseudospinor and the  $P_{6s1/2}(r)$  large component of the spinor from numerical SCF calculation of the  $\dots 4f_{5/2}^5 6s_{1/2}^2 5d_{3/2}^1 (J = 4)$  term for the Sm atom (which differs from the generator state by the occupation number of the  $4f$  shell) and their difference multiplied by 500. The “Breit SCF relaxation” is the (multiplied by 500) difference in  $P_{6s1/2}(r)$  from the all-electron DFB and DF calculations. The “relativistic contraction” is the (multiplied by 5) difference in  $P_{6s1/2}(r)$  from the all-electron DFB calculations with the standard and increased in 1000 times light velocities. Note that the logarithmic scale for  $r$  is used.

the third and fourth columns in Tables 4 and 6 that the accuracy of Gaussian approximation of the numerical GRECP components is high.

The shape of the  $6s$  spinor is very well reproduced in the outercore and valence region with the help of the GRECP (see Figure 2). One can also see that the contraction of the  $6s$  orbital due to the relativistic effects is essential and should be taken into account in accurate calculations whereas the relaxation of the  $6s$  spinor due to inclusion of Breit interactions in the SCF procedure is small. It should be emphasized that the state used in these calculations (Table 6,

Figure 2, splitting into relativistic configurations and terms in Table 4) differs from the generator state by the occupation number of the  $4f$  shell.

## 5. Molecular Calculations

### 5.1. Coupled Cluster Calculations of Adiabatic Potential Curve for Yb Dimer

The properties of the Yb dimer are necessary to assess the feasibility of using laser cooled and trapped Yb atomic species

for ultraprecise optical clocks [6, 7, 39, 89] or quantum information-processing devices [43]. Unfortunately, reliable experimental data on the dissociation energy, equilibrium internuclear distance, and spectroscopic constants of the  $\text{Yb}_2$  molecule are unknown; e.g., the uncertainty of the experimental dissociation energy estimate from paper [34], 0.17 eV, is comparable to the value itself. Calculations of these properties were performed in a series of papers where, in particular, the values of 400 [21], 470 [104], 740 [15],  $500 \div 1400$  [108], and  $724 \text{ cm}^{-1}$  [13] for the dissociation energy of the ground state were reported.

The generated earlier GRECP [94] with 42 explicitly treated electrons for each Yb atom was applied to calculations of the adiabatic potential curve, dissociation energy, equilibrium internuclear distance, and spectroscopic constants for the  $^1\Sigma_g^+$  ground state of the  $\text{Yb}_2$  molecule [61]. The scalar relativistic coupled cluster method with single, double and non-iterative triple cluster amplitudes (CCSD(T)) particularly well suited for closed-shell van-der-Waals systems is used for the correlation treatment. A series of extremely flexible generalized correlation basis sets up to the  $(38, 22, 24, 14, 7, 1)/[11, 10, 9, 7, 5, 1]$  one generated with the help of procedure [59, 65] were used. It was concluded from a series of preliminary calculations that the quality of the basis set is of crucial importance for accurate calculations of the ytterbium dimer. The basis set superposition errors (BSSE) were compensated quite accurately by the counterpoise correction [35, 55] calculated for the Yb  $6s^2$  state with one more Yb atom treated as the ghost one.

The  $^1\Sigma_g^+$  closed-shell ground state of the  $\text{Yb}_2$  molecule dissociates into two closed-shell Yb atoms in the  $4f^{14}6s^2(^1S)$  ground state. The computed ground-state potential energy curves for the  $\text{Yb}_2$  molecule are shown in Figure 3. One can see the essential difference between the CCSD(T) and CCSD(T)+iTQ curves that corresponds to the contribution from the quadruple cluster amplitudes and iteration of the triple ones (iTQ). This contribution

comprises about  $120 \text{ cm}^{-1}$  for the dissociation energy and should be taken into account in accurate calculations. It should be noted that this contribution was neglected in the previous calculations [13, 15, 21, 104]. The difference between the CCSD(T)+iTQ and CCSD(T)+iTQ+SO curves is rather small. It corresponds to the contribution from the spin-orbit (SO) interaction that is about  $20 \text{ cm}^{-1}$  for the dissociation energy. Its smallness can be easily explained by the fact that the SO interaction for the  $\Sigma$ -states in the first order of the perturbation theory gives a zeroth correction for the energy.

The stage of calculation of the molecular constants [57] begins with fitting the numerical potential curve for the dimer by polynomials with the help of the quasi-Hermitian method. Appropriate derivatives of the potential curve at the equilibrium point are calculated by recurrence relations. Then rovibrational Schrödinger equation is solved by the Dunham method to express the Dunham coefficients in terms of these derivatives. Our final results [61] for the dissociation energy, equilibrium internuclear distance, and main spectroscopic constants are  $D_e = 786 \text{ cm}^{-1}$ ,  $R_e = 4.582 \text{ \AA}$ ,  $w_e = 24.1 \text{ cm}^{-1}$ ,  $D_0^0 = 774 \text{ cm}^{-1}$ ,  $B_e = 9.39 \cdot 10^{-3} \text{ cm}^{-1}$ ,  $w_e x_e = 0.23 \text{ cm}^{-1}$ ,  $\alpha_e = 8.3 \cdot 10^{-5} \text{ cm}^{-1}$ , and  $Y_{02} = -5.7 \cdot 10^{-9} \text{ cm}^{-1}$ .

To estimate the computational accuracy of the  $\text{Yb}_2$  calculation, we perform the calculations on the well-studied  $\text{Ca}_2$  molecule [63] which has similar electronic structure. The same computational methods were applied having in mind a reasonable assumption that the errors for similar systems will be close to one another. In contrast to  $\text{Yb}_2$ , rather precise experimental data are available for the  $\text{Ca}_2$  molecule [3, 5, 9, 103]. Our results and the experimental data are in a good agreement that should not be considered as fortuitous coincidence because it is observed not only for one parameter (such as  $D_e$ ) but also for several independent parameters ( $R_e$ ,  $D_e$ ,  $w_e$ ,  $w_e x_e$ ,  $\alpha_e$ ,  $Y_{02}$ ). In particular, the calculated dissociation energy for  $\text{Ca}_2$  has 3% error with respect to the most precise experimental datum [3], whereas the corresponding error for

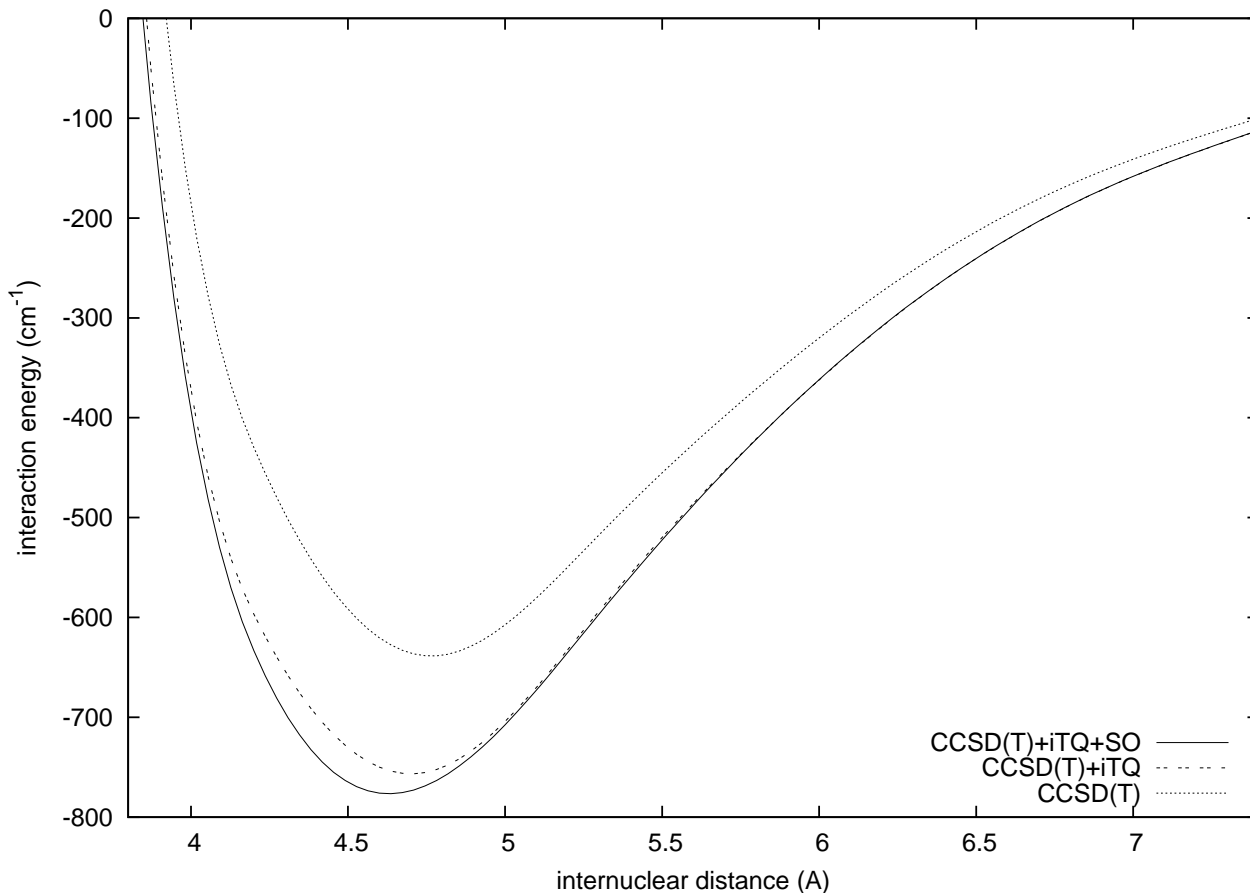


Figure 3. The calculated potential energy functions for the  $\text{Yb}_2$  ground state. The CCSD(T)+iTQ+SO curve corresponds to our best full relativistic results. The CCSD(T)+iTQ curve presents the scalar relativistic results, i.e. without accounting for the spin-orbit interaction. The CCSD(T) curve was obtained with the help of the scalar relativistic coupled cluster method with single, double and non-iterative triple cluster amplitudes (CCSD(T)), i.e. without accounting for the quadruple cluster amplitudes, iteration of the triples (iTQ) and the spin-orbit (SO) interaction.

the equilibrium internuclear distance [103] is only 0.09%.

### 5.2. Correlation Calculations of T,P-odd and Hyperfine Constants for the YbF Molecule

The YbF molecule [40, 41, 90, 91] is one of the operative objects for the experimental search for the break of inversion symmetry (P) and time-reversal invariance (T). The observation of non-zero T,P-odd effects, in particular electron Electric Dipole Moment (eEDM,  $d_e$ ),

would indicate the presence of so-called “new physics” [24] beyond the Standard Model of electroweak and strong interactions [29, 82, 105, 106] that is certainly of fundamental importance. The latest constraint in the experiment with the YbF molecule was  $|d_e| < 1.05 \cdot 10^{-27} e\text{-cm}$  [40], (whereas the stringest bound on the eEDM was obtained on the ThO molecule,  $|d_e| < 9 \cdot 10^{-29} e\text{-cm}$  [8]) where  $e$  is the charge of the electron. Since the experiments continue, their precision is expected to rise by up to an order of magnitude in the near future.

A crucial feature of the experiments to

search T,P-odd effects in atoms, molecules, liquids, or solids is that for interpretation of the measured data in terms of the fundamental constants of the T,P-odd interactions, one must calculate those parameters of the systems, which establish a connection between the measured data and the studied fundamental constants. These T,P-odd parameters are described by operators heavily concentrated near or on heavy nuclei; they cannot be measured and their theoretical study is not a trivial task. It is known, the T,P-odd parameters are sensitive to the spin density in the vicinity of the heavy nucleus (see, e.g., paper [48]). The same, of course, can be said about magnetic hyperfine constants. So, comparison of the calculated constants of the hyperfine structure on the  $^{171}\text{Yb}$  nucleus with the experimental data provides an important test of the quality of the calculation. (The T,P-odd and hyperfine interactions with the  $^{19}\text{F}$  nucleus are significantly smaller and are not of interest.)

The generated earlier GRECP [66, 97, 101] with 10 explicitly treated electrons ( $5s^25p^66s^2$ ) for the Yb atom was used for calculations of the electronic wavefunction of the ground  $^2\Sigma^+$  state of the YbF molecule [60]. The  $4s^24p^64d^{10}4f^{14}$  electrons were not included in the molecular GRECP calculations unlike Section 2. Moreover, the  $5s$  and  $5p$  pseudospinors derived from the calculation on the  $\text{Yb}^{2+}$  cation were “frozen” the use of the level-shift technique [94, 96]. It was necessary to “freeze” these shells because the correlation and polarization effects connected with these and rest innercore electrons were taken into account with the help of the Effective Operator (EO) technique (see paper [47] for details) after the restoration of proper molecular four-component spinors in the innercore region of Yb in the framework of the Non-variational One-Center Restoration (NOCR) procedure [97–99]. The EO for the hyperfine and T,P-odd parameters were constructed by means of the atomic Many Body Perturbation Theory (MBPT) [23] for the  $\text{Yb}^{2+}$  cation. The correlations for 2 valence electrons of Yb and 9 of F were considered in the scalar relativistic

calculations in the framework of the restricted active space SCF (RASSCF) method [74] implemented in MOLCAS program package [4]. Expressions for the  $A$ ,  $A_d$  hyperfine constants and the  $W_d$ ,  $W_S$ ,  $W_A$  T,P-odd parameters can be found in papers [46, 48]. All the atomic radial integrals and four-component spinors were calculated for the finite nucleus  $^{171}\text{Yb}$  using the model of uniform charge distribution within the sphere.

The results of our calculations [60, 97] for the isotropic  $A = (A_{\parallel} + 2A_{\perp})/3$  and dipole  $A_d = (A_{\parallel} - A_{\perp})/3$  hyperfine constants of the YbF molecule are presented in Table 3 where they are compared with the experimental data [30, 86, 102]. The hyperfine constants [30, 86] were measured for the molecule in a molecular beam whereas the experimental data [102] were obtained using an inert gas matrix. The former most closely corresponds both the conditions of the eEDM experiment [40, 41] and the model used in quantum chemical calculations. The latest [30] of two molecular beam experiments has smallest errors. One can see that the GRECP/RASSCF/NOCR/EO hyperfine constants [60] agree at the 10% level with these latest experimental data [30]. Similar accuracy is expected for the T,P-odd parameters that is quite satisfactory for the requirements of the eEDM experiment. (One should remember that only the 10 electron GRECP was applied in the calculations and the computational resources to take into account the correlation effects were strongly restricted about 20 years ago.)

The  $W_d$  parameter describes interaction of the eEDM with the internal molecular electric field. The  $W_d$  values from the four-component all-electron, [2, 11, 28, 68–73, 76, 79, 85] GRECP, [60, 97] and semiempirical [44, 45] calculations are collected in Table 3. At the one-configurational level, the GRECP/SCF/NOCR value [97] is in good agreement with the corresponding all-electron ones, in particular the unpaired valence electron contribution from the unrestricted DF [76] and restricted DF results [2, 69]. However, the restricted DF value [79] is essentially smaller.

When the correlations are taken into account, the GRECP/RASSCF/NOCR/EO value [60] is in good agreement with that of the restricted DF method with core polarization correction by means of MBPT [79], the restricted active space configuration interaction (RASCI) method for the largest number (76) of active orbitals [72] and the relativistic coupled cluster method with single and double cluster amplitudes (RCCSD) [2] with DC Hamiltonian. (The unrestricted DF result [76] are also in perfect agreement.) However, the DC/RASCI result [28] is essentially smaller. Unfortunately, the authors [28] did not calculate the  $A_d$  constant to compare with the experiment. Our value for the effective electric field on the unpaired electron is  $W_d/2 = 4.9$  a.u. =  $2.5 \times 10^{10}$  V cm<sup>-1</sup>.

## Conclusions

The lanthanide compounds are rather difficult objects for accurate quantum chemical calculations due to significant relativistic effects, high density of low-lying electronic states, and complexity of their electronic structure. Relativistic effects including desirably Breit interactions should be taken into account in accurate calculations on lanthanides. The GRECP method allows one to carry out economical and reliable calculations on lanthanide

compounds at the level of the “chemical accuracy”. Breit interactions and other relativistic effects as well as the effects of finite nuclear size are readily and efficiently incorporated into the GRECP model. That allows one to perform high-level relativistic calculations with computationally simpler Coulomb electron-electron interaction operator. The GRECP model can be used not only for the evaluation of “valence-type” properties (for instance, potential surfaces of ground and low-lying excited states, spectroscopic constants) but also for estimating the molecular characteristics that are sensitive to behaviour of valence spinors in the vicinity of heavy atom nucleus. To calculate the latter (“core-type”) properties such as the hyperfine structure constants and T,P-odd parameters, the NOCR technique for four-component wavefunction in the vicinity of heavy nuclei should be applied after the GRECP calculation with smoothed pseudospinors. The generated GRECPs are available at <http://qchem.pnpi.spb.ru/recp.html>

## Acknowledgments

The author is grateful to Prof. Anatoly V. Titov. The reported study was supported by the Russian Science Foundation grant (project No. 14-31-00022).

---

## References

- [1] Abarenkov, I. V. and Heine, V. [1965], ‘The model potential for positive ions’, *Philos. Mag.* **12**(117), 529–537.
- [2] Abe, M., Gopakumar, G., Hada, M., Das, B. P., Tatewaki, H. and Mukherjee, D. [2014], ‘Application of relativistic coupled-cluster theory to the effective electric field in ybf’, *Phys. Rev. A* **90**, 022501.  
**URL:** <http://link.aps.org/doi/10.1103/PhysRevA.90.022501>
- [3] Allard, O., Pashov, A., Knöckel, H. and Tiemann, E. [2002], ‘Ground-state potential of the Ca dimer from fourier transform spectroscopy’, *Phys. Rev. A* **66**, 042503.
- [4] Andersson, K., Blomberg, M. R. A., Fülcher, M. P., Karlström, G., Lindh, R., Malmqvist, P.-A., Neogrády, P., Olsen, J., Roos, B. O., Sadlej, A. J., Schütz, M., Seijo, L., Serrano-Andrés, L., Siegbahn, P. E. M. and Widmark, P.-O. [1999]. Quantum-chemical program package “MOLCAS”, Version 4.1.
- [5] Balfour, W. J. and Whitlock, R. F. [1975], ‘The

- visible absorption spectrum of diatomic calcium', *Can. J. Phys.* **53**, 472–485.
- [6] Barber, Z. W., Hoyt, C. W., Oates, C. W., Hollberg, L., Taichenachev, A. V. and Yudin, V. I. [2006], 'Direct excitation of the forbidden clock transition in neutral  $^{174}\text{Yb}$  atoms confined to an optical lattice', *Phys. Rev. Lett.* **96**, 083002.
- [7] Barber, Z. W., Stalnaker, J. E., Lemke, N. D., Poli, N., Oates, C. W., Fortier, T. M., Diddams, S. A., Hollberg, L. and Hoyt, C. W. [2008], 'Optical lattice induced light shifts in an Yb atomic clock', *Phys. Rev. Lett.* **100**, 103002.
- [8] Baron, J., Campbell, W. C., DeMille, D., Doyle, J. M., Gabrielse, G., Gurevich, Y. V., Hess, P. W., Hutzler, N. R., Kirilov, E., Kozyryev, I., OвѢ<sup>TM</sup>Leary, B. R., Panda, C. D., Parsons, M. F., Petrik, E. S., Spaun, B., Vutha, A. C. and West, A. D. [2014], 'Order of magnitude smaller limit on the electric dipole moment of the electron', *Science* **343**(6168), 269–272.
- [9] Bondybey, V. E. and English, J. H. [1984], 'Laser-induced fluorescence of the calcium dimer in supersonic jet: the red spectrum of  $\text{Ca}_2^+$ ', *Chem. Phys. Lett.* **111**, 195–200.
- [10] Bonifacic, V. and Huzinaga, S. [1974], 'Atomic and molecular calculations with the model potential method. I', *J. Chem. Phys.* **60**(7), 2779–2786.
- [11] Borschevsky, A., Ilias, M., Dzuba, V. A., Beloy, K., Flambaum, V. V. and Schwerdtfeger, P. [2012], 'P-odd interaction constant  $w_a$  from relativistic *ab initio* calculations of diatomic molecules', *Phys. Rev. A* **85**, 052509.
- [12] Bratzev, V. F., Deyneka, G. B. and Tupitsyn, I. I. [1977], 'Application of the Hartree-Fock method to calculation of relativistic atomic wave functions', *Bull. Acad. Sci. USSR, Phys. Ser.* **41**(12), 173–182.
- [13] Buchachenko, A. A., Chalasinski, G. and Szczesniak, M. M. [2007], 'Interaction of lanthanide atoms: Comparative *ab initio* study of  $\text{YbHe}$ ,  $\text{Yb}_2$  and  $\text{TmHe}$ ,  $\text{TmYb}$  potentials', *Eur. Phys. J. D* **45**, 147–153.
- [14] Bunzli, J.-C. G. and Piguet, C. [2005], 'Taking advantage of luminescent lanthanide ions', *Chem. Soc. Rev.* **34**, 1048–1077.
- [15] Cao, X. and Dolg, M. [2002], 'Pseudopotential study of lanthanum and lutetium dimers', *Theor. Chem. Acc.* **108**, 143–149.
- [16] Christiansen, P. A., Lee, Y. S. and Pitzer, K. S. [1979], 'Improved *ab initio* effective core potentials for molecular calculations', *J. Chem. Phys.* **71**(11), 4445–4450.
- [17] Cundari, T. R., Sommerer, S. O., Strohecker, L. A. and Tippett, L. [1995], 'Effective core potential studies of lanthanide complexes', *J. Chem. Phys.* **103**(4), 7058–7063.
- [18] Cundari, T. R. and Stevens, W. J. [1993], 'Effective core potential methods for the lanthanides', *J. Chem. Phys.* **98**(4), 5555–5565.
- [19] Doi, K., Fujitani, K., Kadowaki, N., Nakamura, K., Tachibana, A. and Hattori, T. [2005], 'Structures and electronic states of gadolinium oxide clusters', *Jpn. J. Appl. Phys.* **44**, 6115–6123.
- [20] Dolg, M., Stoll, H. and Preuss, H. [1989], 'Energy-adjusted *ab initio* pseudopotentials for the rare earth elements', *J. Chem. Phys.* **90**, 1730–1734.
- [21] Dolg, M., Stoll, H. and Preuss, H. [1992], 'Homonuclear diatomic lanthanoid compounds: a pseudopotential configuration interaction and correlation energy density functional study', *J. Mol. Struct. (Theochem)* **277**, 239–249.
- [22] Douglas, M. and Kroll, N. M. [1974], 'Quantum electro-dynamical corrections to the fine structure of helium', *Ann. Phys.* **82**, 89–155.
- [23] Dzuba, V. A., Flambaum, V. V. and Kozlov, M. G. [1996], 'Calculation of energy levels for atoms with several valence electrons', *JETP Lett.* **63**(11), 882–887.
- [24] Erler, J. and Ramsey-Musolf, M. J. [2005], 'Low energy tests of the weak interaction', *Prog. Part. Nucl. Phys.* **54**, 351–442.
- [25] Ermler, W. C., Lee, Y. S., Pitzer, K. S. and Winter, N. W. [1978], '*Ab initio* effective core potentials including relativistic effects. II. Potential energy curves for  $\text{Xe}_2$ ,  $\text{Xe}_2^+$ , and  $\text{Xe}_2^*$ ', *J. Chem. Phys.* **69**(3), 976–983.
- [26] Ermler, W. C., Ross, R. B. and Christiansen, P. A. [1988], 'Spin-orbit coupling and other relativistic effects in atoms and molecules', *Adv. Quantum Chem.* **19**, 139–182.
- [27] Flambaum, V. V. [2006], 'Enhanced effect of temporal variation of the fine structure constant in diatomic molecules', *Phys. Rev. A* **73**, 034101. [arXiv: physics/0601034].
- [28] Fukuda, M., Soga, K., Senami, M. and Tachibana, A. [2016], 'Local spin dynamics with the electron electric dipole moment', *J. Mol. Spectrosc.* **93**, 012518.
- [29] Glashow, S. L. [1961], 'Partial-symmetries of weak interactions', *Nuclear Physics* **22**, 579–588.
- [30] Glassman, Z., Mawhorter, R., Grabow, J.-U., Le,

- A. and Steimle, T. C. [2014], ‘The hyperfine interaction in the odd isotope of ytterbium fluoride,  $^{171}\text{YbF}$ ’, *J. Mol. Spectrosc.* **300**, 7–11.
- [31] Goddard III, W. A. [1968], ‘New foundation for the use of pseudopotentials in metals’, *Phys. Rev.* **174**(3), 659–662.
- [32] Gopakumar, G., Abe, M., Das, B. P., Hada, M. and Hirao, K. [2010], ‘Relativistic calculations of ground and excited states of  $\text{YbF}$  molecule for ultracold photoassociation spectroscopy studies’, *J. Chem. Phys.* **133**, 124317.
- [33] Grant, I. P. and Quiney, H. M. [2000], ‘Application of relativistic theories and quantum electrodynamics to chemical problems’, *Int. J. Quantum Chem.* **80**, 283–297.
- [34] Guido, M. and Balducci, G. [1972], ‘Dissociation energy of  $\text{Yb}_2$ ’, *J. Chem. Phys.* **57**, 5611–5612.
- [35] Gutowski, M., van Lenthe, J. H., Verbeek, J., van Duijneveldt, F. B. and Chalański, G. [1986], ‘The basis set superposition error in correlated electronic structure calculations’, *Chem. Phys. Lett.* **124**(4), 370–375.
- [36] Hafner, P. and Schwarz, W. H. E. [1979], ‘Molecular spinors from the quasi-relativistic pseudopotential approach’, *Chem. Phys. Lett.* **65**(3), 537–541.
- [37] Heine, V. and Abarenkov, I. V. [1964], ‘A new method for the electronic structure of metals’, *Philos. Mag.* **9**(99), 451–465.
- [38] Hess, B. A. [1986], ‘Relativistic electronic-structure calculations employing a two-component no-pair formalism with external-field projection operators’, *Phys. Rev. A* **33**(6), 3742–3748.
- [39] Hoyt, C. W., Barber, Z. W., Oates, C. W., Fortier, T. M., Diddams, S. A. and Hollberg, L. [2005], ‘Observation and absolute frequency measurements of the  $^1s_0 - ^3p_0$  optical clock transition in neutral ytterbium’, *Phys. Rev. Lett.* **95**, 083003.
- [40] Hudson, J. J., Kara, D. M., Smallman, I. J., Sauer, B. E., Tarbutt, M. R. and Hinds, E. A. [2011], ‘Improved measurement of the shape of the electron’, *Nature* **473**, 493–496.
- [41] Hudson, J. J., Sauer, B. E., Tarbutt, M. R. and Hinds, E. A. [2002], ‘Measurement of the electron electric dipole moment using  $\text{YbF}$  molecules’, *Phys. Rev. Lett.* **89**(2), 023003.
- [42] Isaev, T. A., Mosyagin, N. S., Kozlov, M. G., Titov, A. V., Eliav, E. and Kaldor, U. [2000], ‘Accuracy of RCC-SD and PT2/CI methods in all-electron and RECP calculations on Pb and  $\text{Pb}^{2+}$ ’, *J. Phys. B* **33**(22), 5139–5149.
- [43] Kotochigova, S. and Julienne, P. [2003], Potential energy surface database of group II dimer molecules, in ‘<http://www.nist.gov/physlab/data/pes/index.cfm>’.
- [44] Kozlov, M. G. [1997], ‘Enhancement of the electric dipole moment of the electron in the  $\text{YbF}$  molecule’, *J. Phys. B* **30**, L607–612.
- [45] Kozlov, M. G. and Ezhov, V. F. [1994], ‘Enhancement of the electric dipole moment of the electron in the  $\text{YbF}$  molecule’, *Phys. Rev. A* **49**(6), 4502–4506.
- [46] Kozlov, M. G., Fomichev, V. I., Dmitriev, Yu. Yu., Labzovsky, L. N. and Titov, A. V. [1987], ‘Calculation of the P- and T-odd spin-rotational Hamiltonian of the  $\text{PbF}$  molecule’, *J. Phys. B* **20**(19), 4939–4948.
- [47] Kozlov, M. G., Titov, A. V., Mosyagin, N. S. and Souchko, P. V. [1997], ‘Enhancement of the electric dipole moment of the electron in the  $\text{BaF}$  molecule’, *Phys. Rev. A* **56**(5), R3326–3329.
- [48] Kozlov, M. and Labzovsky, L. [1995], ‘Parity violation effects in diatomics’, *J. Phys. B* **28**(9), 1933–1961.
- [49] Labzovsky, L. N. and Goidenko, I. [2002], QED theory of atoms, in P. Schwerdtfeger, ed., ‘Relativistic Electronic Structure Theory. Part I. Fundamentals’, Elsevier, Amsterdam, pp. 401–467.
- [50] Lamoreaux, S. K. [2002], ‘Solid-state systems for the electron electric dipole moment and other fundamental measurements’, *Phys. Rev. A* **66**(2), 022109.
- [51] Lanza, G. and Fragala, I. L. [1996], ‘A relativistic effective core potential ab initio study of molecular geometries and vibrational frequencies of lanthanide trihalides  $\text{LnX}_3$  ( $\text{Ln}=\text{gd,lu}$ ;  $\text{x}=\text{f,cl}$ )’, *Chem. Phys. Lett.* **255**, 341–346.
- [52] Lanza, G. and Minichino, C. [2004], ‘Ab initio study on spectroscopic properties of  $\text{gdF}_3$  and  $\text{gdCl}_3$ ’, *J. Phys. Chem. A* **108**, 4949–4960.
- [53] Lee, Y. S., Ermler, W. C. and Pitzer, K. S. [1977], ‘Ab initio effective core potentials including relativistic effects. I. Formalism and applications to the Xe and Au atoms’, *J. Chem. Phys.* **67**(12), 5861–5876.
- [54] Lindroth, E., Mårtensson-Pendrill, A.-M., Ynnerman, A. and Öster, P. [1989], ‘Self-consistent treatment of the Breit interaction with application to the electric dipole moment in thallium’, *J. Phys. B* **22**, 2447–2464.
- [55] Liu, B. and McLean, A. D. [1989], ‘The

- interacting correlated fragments model for weak interactions, basis set superposition error, and the helium dimer potential', *J. Chem. Phys.* **91**(4), 2348–2359.
- [56] Marquardt, D. W. [1963], 'An algorithm for least-squares estimation of nonlinear parameters', *J. Soc. Indust. Appl. Math.* **11**(2), 431–441.
- [57] Mitin, A. V. [1998], 'Calculation of rovibrational energy levels of diatomic molecules by Dunham method with potential obtained from ab initio calculations', *J. Comput. Chem.* **19**(1), 94–101.
- [58] Mohr, P. J. [1997], 'QED corrections in heavy atoms', *Phys. Rep.* **293**, 227–369.
- [59] Mosyagin, N. S., Eliav, E., Titov, A. V. and Kaldor, U. [2000], 'Comparison of relativistic effective core potential and all-electron Dirac-Coulomb calculations of mercury transition energies by the relativistic coupled-cluster method', *J. Phys. B* **33**(4), 667–676.
- [60] Mosyagin, N. S., Kozlov, M. G. and Titov, A. V. [1998], 'Electric dipole moment of the electron in the YbF molecule', *J. Phys. B* **31**(19), L763–767.
- [61] Mosyagin, N. S., Petrov, A. N. and Titov, A. V. [2011], 'The effect of the iterative triple and quadruple cluster amplitudes on the adiabatic potential curve in the coupled cluster calculations of the ground electronic state of the Yb dimer', *Int. J. Quantum Chem.* **111**, 3793–3798.
- [62] Mosyagin, N. S., Petrov, A. N., Titov, A. V. and Tupitsyn, I. I. [2006], GRECPs accounting for Breit effects in uranium, plutonium and superheavy elements 112, 113, 114, in J.-P. Julien, J. Maruani, D. Mayou, S. Wilson and G. Delgado-Barrio, eds, 'Recent Advances in the Theory of Chemical and Physical Systems', Vol. B 15 of *Progr. Theor. Chem. Phys.*, Springer, Dordrecht, The Netherlands, pp. 229–251.
- [63] Mosyagin, N. S., Petrov, A. N., Titov, A. V. and Zaitsevskii, A. V. [2013], 'Generalized relativistic effective core potential calculations of the adiabatic potential curve and spectroscopic constants for the ground electronic state of the  $ca_2$  molecule', *Int. J. Quantum Chem.* **1113**, 2277–2281.
- [64] Mosyagin, N. S. and Titov, A. V. [n.d.], Comment on "Accurate relativistic effective potentials for the sixth-row main group elements" [J.Chem.Phys., v.107, 9975 (1997)]. arXiv.org/physics/9808006 (1998).
- [65] Mosyagin, N. S., Titov, A. V., Eliav, E. and Kaldor, U. [2001], 'Generalized relativistic effective core potential and relativistic coupled cluster calculation of the spectroscopic constants for the HgH molecule and its cation', *J. Chem. Phys.* **115**(5), 2007–2013.
- [66] Mosyagin, N. S., Titov, A. V. and Latajka, Z. [1997], 'Generalized relativistic effective core potential: Gaussian expansions of potentials and pseudospinors for atoms Hg through Rn', *Int. J. Quantum Chem.* **63**(6), 1107–1122.
- [67] Mosyagin, N. S., Zaitsevskii, A. V., Skripnikov, L. V. and Titov, A. V. [2016], 'Generalized relativistic effective core potentials for actinides', *Int. J. Quantum Chem.* **116**(4), 301–315.
- [68] Naik, D., Sikarwar, M., Nayak, M. K. and Ghosh, S. K. [2014], 'Re-appraisal of the hyperfine-structure constants in ybf: relativistic configuration interaction approach', *J. Phys. B* **47**, 225103.
- [69] Nayak, M. K. and Chaudhuri, R. K. [2006], 'Ab initio calculation of P,T-odd effects in YbF molecule', *Chem. Phys. Lett.* **419**(1-3), 191–194.
- [70] Nayak, M. K. and Chaudhuri, R. K. [2007], 'Perturbative calculations of p,t-odd effects in heavy polar diatomic molecules', *J. Phys. Conf. Ser.* **80**, 012051.
- [71] Nayak, M. K. and Chaudhuri, R. K. [2008], 'Calculation of the electron-nucleus scalar-pseudoscalar interaction constant  $w_s$  for ybf and baf molecules: A perturbative approach', *Phys. Rev. A* **78**, 012506.
- [72] Nayak, M. K. and Chaudhuri, R. K. [2009], 'Re-appraisal of the P,T-odd interaction constant  $w_d$  in ybf: relativistic configuration interaction approach', *Pramana* **73**(3), 581 – 586.
- [73] Nayak, M. K., Chaudhuri, R. K. and Das, B. P. [2007], 'Ab initio calculation of the electron-nucleus scalar-pseudoscalar interaction constant  $w_s$  in heavy polar molecules', *Phys. Rev. A* **75**, 022510.
- [74] Olsen, J. and Roos, B. O. [1988], 'Determinant based configuration interaction algorithms for complete and restricted configuration interaction spaces', *J. Chem. Phys.* **89**(4), 2185–2192.
- [75] Pacios, L. F. and Christiansen, P. A. [1985], 'Ab initio relativistic effective potentials with spin-orbit operators. I. Li through Ag', *J. Chem. Phys.* **82**(6), 2664–2671.
- [76] Parpia, F. [1998], 'Ab initio calculation of the enhancement of the EDM of an electron in the YbF', *J. Phys. B* **31**, 1409–1430.
- [77] Petrov, A. N., Mosyagin, N. S., Titov, A. V. and Tupitsyn, I. I. [2004], 'Accounting for the Breit

- interaction in relativistic effective core potential calculations of actinides', *J. Phys. B* **37**, 4621–4637.
- [78] Quiney, H. M., Grant, I. P. and Wilson, S. [1987], 'The Dirac equation in the algebraic approximation: V. Self-consistent field studies including the Breit interaction', *J. Phys. B* **20**(7), 1413–1422.
- [79] Quiney, H. M., Skaane, H. and Grant, I. P. [1998], 'Hyperfine and P,T-odd effects in YbF  $^2\Sigma$ ', *J. Phys. B* **31**, L85–95.
- [80] Reiher, M. and Hess, B. A. [2000], Relativistic electron-structure calculations for atoms and molecules, in J. Grotendorst, ed., 'Modern Methods and Algorithms of Quantum Chemistry', Vol. 1, Jülich, pp. 451–477. [<http://www.fz-juelich.de/nic-series>].
- [81] Ross, R. B., Gayen, S. and Ermler, W. C. [1994], 'Ab initio relativistic effective potentials with spin-orbit operators. V. Ce through Lu', *J. Chem. Phys.* **100**(11), 8145–8155.
- [82] Salam, A. [1968], Weak and electromagnetic interactions, in N. Svartholm, ed., 'Elementary particle theory, relativistic groups, and analyticity', Almqvist and Wiksells, Stockholm, Sweden, pp. 367–377.
- [83] Seijo, L. and Barandiarán, Z. [2004], Relativistic ab-initio model potential calculations for molecules and embedded clusters, in P. Schwerdtfeger, ed., 'Relativistic Electronic Structure Theory. Part 2. Applications', Elsevier, Amsterdam, pp. 417–475.
- [84] Shabaev, V. M. [2002], 'Two-time Green's function method in quantum electrodynamics of high- $Z$  few-electron atoms', *Phys. Rep.* **356**, 119–228.
- [85] Sikarwar, M., Nayak, M. K. and Ghosh, S. K. [2013], 'Ab initio calculation of the p-odd interaction constant  $w_a$  in ybf: a relativistic configuration-interaction approach', *J. Phys. B* **46**, 175102.
- [86] Steimle, T. C., Ma, T. and Linton, C. [2007], 'The hyperfine interaction in the  $A$   $^2\Pi_{1/2}$  and  $X$   $^2\Sigma^+$  states of ytterbium monofluoride', *J. Chem. Phys.* **127**, 234316. Errata: *J. Chem. Phys.* **128**, 209903 (2008); *J. Chem. Phys.* **137**, 109901 (2012).
- [87] Stoll, H., Metz, B. and Dolg, M. [2002], 'Relativistic energy-consistent pseudopotentials – recent results', *J. Comput. Chem.* **23**, 767–778.
- [88] Sushkov, A. O., Eckel, S. and Lamoreaux, S. K. [2010], 'Prospects for an electron electric-dipole moment search with ferroelectric (eu,ba)tio3 ceramics', *Phys. Rev. A* **81**, 022104.
- [89] Taichenachev, A. V., Yudin, V. I., Oates, C. W., Hoyt, C. W., Barber, Z. W. and Hollberg, L. [2006], 'Magnetic field-induced spectroscopy of forbidden optical transitions with application to lattice-based optical atomic clocks', *Phys. Rev. Lett.* **96**, 083001.
- [90] Tarbutt, M. R., Bethlem, H. L., Hudson, J. J., Ryabov, V. L., Ryzhov, V. A., Sauer, B. E., Meijer, G. and Hinds, E. A. [2004], 'Slowing heavy ground state molecules using an alternating ground state decelerator', *Phys. Rev. Lett.* **92**, 173002.
- [91] Tarbutt, M. R., Hudson, J. J., Sauer, B. E., Hinds, E. A., Ryzhov, V. A., Ryabov, V. L. and Ezhov, V. F. [2002], 'A jet beam source of cold YbF radicals', *J. Phys. B* **35**(24), 5013–5022.
- [92] Titov, A. V., Mitrushenkov, A. O. and Tupitsyn, I. I. [1991], 'Effective core potential for pseudo-orbitals with nodes', *Chem. Phys. Lett.* **185**(3,4), 330–334.
- [93] Titov, A. V. and Mosyagin, N. S. [1995], 'Self-consistent relativistic effective core potentials for transition metal atoms: Cu, Ag, and Au', *Structural Chem.* **6**(4/5), 317–321.
- [94] Titov, A. V. and Mosyagin, N. S. [1999], 'Generalized relativistic effective core potential: Theoretical grounds', *Int. J. Quantum Chem.* **71**(5), 359–401.
- [95] Titov, A. V. and Mosyagin, N. S. [2000], 'The generalized relativistic effective core potential method: Theory and calculations', *Russ. J. Phys. Chem.* **74**, Suppl.2, S376–387. [arXiv: physics/0008160].
- [96] Titov, A. V., Mosyagin, N. S., Alekseyev, A. B. and Buenker, R. J. [2001], 'GRECP/MRD-CI calculations of spin-orbit splitting in ground state of Tl and of spectroscopic properties of TlH', *Int. J. Quantum Chem.* **81**(6), 409–421.
- [97] Titov, A. V., Mosyagin, N. S. and Ezhov, V. F. [1996], ' $P, T$ -odd spin-rotational Hamiltonian for the YbF molecule', *Phys. Rev. Lett.* **77**(27), 5346–5349.
- [98] Titov, A. V., Mosyagin, N. S., Petrov, A. N. and Isaev, T. A. [2005], 'Two-step method for precise calculation of core properties in molecules', *Int. J. Quantum Chem.* **104**(2), 223–239.
- [99] Titov, A. V., Mosyagin, N. S., Petrov, A. N., Isaev, T. A. and DeMille, D. P. [2006], Study of P,T-parity violation effects in polar heavy-atom molecules, in J.-P. Julien, J. Maruani,

- D. Mayou, S. Wilson and G. Delgado-Barrio, eds, 'Recent Advances in the Theory of Chemical and Physical Systems', Vol. B 15 of *Progr. Theor. Chem. Phys.*, Springer, Dordrecht, The Netherlands, pp. 253–283.
- [100] Tsuchiya, T., Taketsugu, T., Nakano, H. and Hirao, K. [1999], 'Theoretical study of electronic and geometric structures of a series of lanthanide trihalides  $\text{LnX}_3$  (Ln=La, Ce, Pr, Nd, Sm, Eu, Gd, Tb, Dy, Ho, Er, Tm, Yb, Lu; X=Cl, F)', *J. Mol. Struct. (Theochem)* **461–462**, 203–222.
- [101] Tupitsyn, I. I., Mosyagin, N. S. and Titov, A. V. [1995], 'Generalized relativistic effective core potential. I. Numerical calculations for atoms Hg through Bi', *J. Chem. Phys.* **103**(15), 6548–6555.
- [102] Van Zee, R. J., Seely, M. L., DeVore, T. C. and Weltner, W. [1978], 'Electron spin resonance of the ytterbium fluoride molecule at 4 K', *J. Phys. Chem.* **82**(10), 1192–1194.
- [103] Vidal, C. R. [1980], 'The molecular constants and potential energy curves of the  $\text{Ca}_2$   $A^1\Sigma_u^+ - X^1\Sigma_g^+$ ', *J. Chem. Phys.* **72**, 1864–1874.
- [104] Wang, Y. and Dolg, M. [1998], 'Pseudopotential study of the ground and excited states of  $\text{Yb}_2^*$ ', *Theor. Chim. Acta* **100**, 124–133.
- [105] Weinberg, S. [1967], 'A model of leptons', *Phys. Rev. Lett.* **19**(21), 1264–1266.
- [106] Weinberg, S. [1972], 'Effects of a neutral intermediate boson in semileptonic processes', *Phys. Rev. D* **5**(6), 1412–1417.
- [107] Woodruff, D. N., Winpenny, R. E. P. and Layfield, R. A. [2013], 'Lanthanide single-molecule magnets', *Chem. Rev.* **113**, 5110–5148.
- [108] Wu, Z. J., Shi, J. S., Zhang, S. Y. and Zhang, H. J. [2004], 'Density-functional study of lanthanum, ytterbium, and lutetium dimers', *Phys. Rev. A* **69**, 064502.
- [109] Zhang, P., Sadeghpour, H. R. and Dalgarno, A. [2010], 'Structure and spectroscopy of ground and excited states of  $\text{LiYb}$ ', *J. Chem. Phys.* **133**, 044306.

Table 1. Transition energies (TE, in  $\text{cm}^{-1}$ ) between the relativistic terms and the states averaged over the nonrelativistic and relativistic configurations of the Sm atom from numerical DFB calculations and the corresponding absolute errors of their reproducing in the different versions of all-electron calculations.

State	DFB	DFB	DF+B	DF	HF
	$A = 150$	$A = 0$	$A = 150$	$A = 150$	$A = 150$
	Fermi	Point	Fermi	Fermi	Fermi
	TE		Absolute errors		
Nonrel.aver. ... $4f^5 6s^2 5d^1 \rightarrow$					
... $4f^5 6s^1 5d^2$	9469	7	0	71	-7115
... $4f^5 6s^2 6p^1$	11992	-4	0	-96	6899
... $4f^5 6s^1 5d^1 6p^1$	14348	5	0	2	-2648
... $4f^6 6s^2$	341	10	1	752	-26152
... $4f^6 6s^1 6p^1$	12949	14	1	753	-28252
... $4f^6 6s^1 5d^1$	14385	15	1	804	-31863
Rel.aver. ... $4f_{5/2}^6 6s_{1/2}^2 \rightarrow$					
... $4f_{5/2}^5 4f_{7/2}^1 6s_{1/2}^2$	20159	-1	1	365	-2417
... $4f_{5/2}^4 4f_{7/2}^2 6s_{1/2}^2$	34691	-1	2	695	-5275
... $4f_{5/2}^3 4f_{7/2}^3 6s_{1/2}^2$	43538	-1	3	986	-8536
... $4f_{5/2}^2 4f_{7/2}^4 6s_{1/2}^2$	46667	-1	3	1237	-12176
... $4f_{5/2}^1 4f_{7/2}^5 6s_{1/2}^2$	44074	-1	3	1445	-16174
... $4f_{7/2}^6 6s_{1/2}^2$	35777	-1	4	1611	-20516
Rel.aver. ... $4f_{5/2}^5 6s_{1/2}^2 5d_{3/2}^1 \rightarrow$					
... $4f_{5/2}^5 6s_{1/2}^2 5d_{5/2}^1$	5505	0	0	57	-1492
Rel.aver. ... $4f_{5/2}^5 6s_{1/2}^2 6p_{1/2}^1 \rightarrow$					
... $4f_{5/2}^5 6s_{1/2}^2 6p_{3/2}^1$	2345	0	0	24	-2098
... $4f_{5/2}^5 6s_{1/2}^2 5d_{3/2}^1 (J = 4) \rightarrow$					
... ( $J = 3$ )	5167	0	0	-1	4
... ( $J = 2$ )	1943	0	0	-8	5
... ( $J = 1$ )	6071	0	0	18	-629

Table 2. The one-electron energies and average radii (in a.u.) for the spinors from numerical DFB calculation of the state of the Sm atom averaged over the nonrelativistic ...  $4f^66s^2$  configuration.

Spinor	One-el. energy	Average radius
$3s_{1/2}$	64.6	0.254
$3p_{1/2}$	57.8	0.244
$3p_{3/2}$	53.3	0.256
$3d_{3/2}$	41.7	0.228
$3d_{5/2}$	40.8	0.232
$4s_{1/2}$	13.7	0.580
$4p_{1/2}$	11.0	0.595
$4p_{3/2}$	9.98	0.622
$4d_{3/2}$	5.55	0.667
$4d_{5/2}$	5.37	0.678
$5s_{1/2}$	1.97	1.44
$5p_{1/2}$	1.17	1.62
$5p_{3/2}$	1.03	1.71
$4f_{5/2}$	0.428	0.945
$4f_{7/2}$	0.409	0.958
$6s_{1/2}$	0.179	4.65

Table 3. The  $A = (A_{\parallel} + 2A_{\perp})/3$  isotropic and  $A_d = (A_{\parallel} - A_{\perp})/3$  dipole hyperfine structure constants and  $W_d$ ,  $W_A$ , and  $W_S$  T,P-odd parameters for the  $^{171}\text{YbF}$  molecule.

Method	$A$ (MHz)	$A_d$ (MHz)	$W_d$ ( $10^{25} \frac{\text{Hz}}{\text{e}\cdot\text{cm}}$ )	$W_A$ (Hz)	$W_S$ (kHz)
Experiment (matrix, 1978) [102] <sup>a</sup>	7617±5	102±3			
(Kozlov, 1994) Semiempirical calculation [45] <sup>a</sup>			-1.5	730	-48
Semiempirical calculation (with 4 <i>f</i> -correction) [44] <sup>a</sup>			-1.26		-43
Experiment (beam, 2007) [86] <sup>b</sup>	7259±21	85±43			
Experiment (beam, 2014) [30] <sup>b</sup>	7273±11	91.1±0.1			
(Titov, 1996) GRECP/SCF/NOCR [97]	4932	59	-0.91	484	-33
GRECP/RASSCF/NOCR [97]	4854	60	-0.91	486	-33
(Quiney, 1998) Restricted DF [79]	5918	35	-0.62 <sup>c</sup>	326 <sup>c</sup>	-22 <sup>c</sup>
Rescaled restricted DF [79]			-1.24 <sup>cd</sup>	652 <sup>cd</sup>	-44 <sup>cd</sup>
Restricted DF + core polarization [79]	7865	60	-1.20 <sup>c</sup>	620 <sup>c</sup>	-42 <sup>c</sup>
(Parpia, 1998) Unrestricted DF (unpaired valence electron) [76]			-0.962		
Unrestricted DF [76]			-1.203		-44 <sup>c</sup>
GRECP/RASSCF/NOCR/EO (Mosyagin, 1998) [60]	7842	79	-1.206	634	
GRECP/RASSCF/NOCR/EO (with 4 <i>f</i> -correction) [60]	7839	94	-1.206	634	
(Borschevsky, 2012) Restricted DF [11]				527	
(DF+DFT)/2 + core polarization [11] <sup>e</sup>				602	
(Nayak, 2006-2014)					
Restricted DF [68, 69, 73, 85]	5713	70	-0.963	475	-34.2
DC/MBPT2 (86 active orbitals) [70]			-1.043		
DC/MBPT2 (96 active orbitals) [71]					-37.1
DC/RASCI (56 active orbitals) [69]			-1.088		
DC/RASCI (76 active orbitals) [72]			-1.164		
DC/RASCI (86 active orbitals) [73, 85]				543	-41.2
DC/RASCI (106 active orbitals) [68]	6725	86			
(Abe, 2014) Restricted DF [2]			-0.88		
DC/RCCSD [2]			-1.12		
(Fukuda, 2016) DC/RASCI [28]			-1.01		

<sup>a</sup>The hyperfine constants [102] were measured for the molecule in an inert gas matrix and the semiempirical T,P-odd parameters [44, 45] were based on these data.

<sup>b</sup>The hyperfine constants [30, 86] were measured for the molecule in a molecular beam.

<sup>c</sup>The results of Quiney, et al. [79] and Parpia [76] have been adjusted by a factor of two to be consistent with the definition of the T,P-odd parameters used in the present paper.

<sup>d</sup>The T,P-odd parameters are rescaled from the “restricted DF” results employing the calculated and experimental  $A$  and  $A_d$  values by the factor  $\sqrt{(A^{\text{expt}} \cdot A_d^{\text{expt}})/(A^{\text{calc}} \cdot A_d^{\text{calc}})}$ , which are in good agreement with the “restricted DF + core polarization” values.

<sup>e</sup>The average of the DF and density functional theory (DFT) results corrected for the core polarization.

Table 4. Transition energies (TE, in  $\text{cm}^{-1}$ ) between the relativistic terms and the states averaged over the nonrelativistic and relativistic configurations of the Sm atom from numerical DFB calculations and the corresponding absolute errors of their reproducing in calculations with different GRECP versions.

State	DFB	Original	Original	Valence	Core	Core
	$A = 150$ Fermi	GRECP (num.)	GRECP (gauss.)	GRECP	GRECP	GRECP
TE	Absolute errors					
Nonrel.aver. ... $4f^5 6s^2 5d^1 \rightarrow$						
... $4f^5 6s^1 5d^2$	9469	-4	-4	-16	-53	-957
... $4f^5 6s^2 6p^1$	11992	8	7	20	33	-467
... $4f^5 6s^1 5d^1 6p^1$	14348	1	1	-8	-38	-1396
... $4f^6 6s^2$	341	-60	-62	-1032	-1056	1526
... $4f^6 6s^1 6p^1$	12949	-60	-62	-1042	-1093	320
... $4f^6 6s^1 5d^1$	14385	-62	-63	-1028	-1085	642
Rel.aver. ... $4f_{5/2}^6 6s_{1/2}^2 \rightarrow$						
... $4f_{5/2}^5 4f_{7/2}^1 6s_{1/2}^2$	20159	105	106	256	256	11
... $4f_{5/2}^4 4f_{7/2}^2 6s_{1/2}^2$	34691	175	178	451	450	13
... $4f_{5/2}^3 4f_{7/2}^3 6s_{1/2}^2$	43538	210	214	583	582	2
... $4f_{5/2}^2 4f_{7/2}^4 6s_{1/2}^2$	46667	208	213	651	649	-22
... $4f_{5/2}^1 4f_{7/2}^5 6s_{1/2}^2$	44074	169	175	655	652	-59
... $4f_{7/2}^6 6s_{1/2}^2$	35777	94	102	596	592	-109
Rel.aver. ... $4f_{5/2}^5 6s_{1/2}^2 5d_{3/2}^1 \rightarrow$						
... $4f_{5/2}^5 6s_{1/2}^2 5d_{5/2}^1$	5505	219	219	179	181	234
Rel.aver. ... $4f_{5/2}^5 6s_{1/2}^2 6p_{1/2}^1 \rightarrow$						
... $4f_{5/2}^5 6s_{1/2}^2 6p_{3/2}^1$	2345	21	21	20	23	535
... $4f_{5/2}^5 6s_{1/2}^2 5d_{3/2}^1 (J = 4) \rightarrow$						
... ( $J = 3$ )	5167	92	92	66	67	106
... ( $J = 2$ )	1943	21	21	12	13	24
... ( $J = 1$ )	6071	341	341	267	269	412

Table 5. The  $\langle r^2 \rangle$  ME (in a.u.) obtained with the spinors from numerical DFB calculations of the state averaged over the nonrelativistic  $4f^5 5d^1 6s^1 6p^1$  configuration (which differs from the generator state by the occupation number of the  $4f$  shell) of the Sm atom and the corresponding relative errors (in %) of their reproducing in different versions of all-electron calculations.

Spinor	DFB	DFB	DF	HF
	$A = 150$ Fermi	$A = 0$ Point	$A = 150$ Fermi	$A = 150$ Fermi
	ME	Relative errors (in %)		
$4s_{1/2}$	0.377586	-0.012	-0.141	10.895
$4p_{1/2}$	0.400820	0.000	-0.259	10.999
$4p_{3/2}$	0.437398	0.001	-0.172	1.717
$4d_{3/2}$	0.510444	0.001	-0.131	1.202
$4d_{5/2}$	0.525484	0.001	-0.066	-1.694
$4f_{5/2}$	0.991432	0.004	0.211	-8.419
$4f_{7/2}$	1.01195	0.004	0.344	-10.276
$5s_{1/2}$	2.23285	-0.013	-0.135	11.352
$5p_{1/2}$	2.79755	0.000	-0.261	11.919
$5p_{3/2}$	3.10529	0.001	-0.155	0.827
$5d_{3/2}$	8.19197	0.007	0.031	-6.702
$5d_{5/2}$	8.49997	0.007	0.124	-10.083
$6s_{1/2}$	20.1753	-0.016	-0.082	12.098
$6p_{1/2}$	37.2712	0.003	-0.198	7.914
$6p_{3/2}$	40.7918	0.004	-0.106	-1.399

Table 6. The  $\langle r^2 \rangle$  ME (in a.u.) obtained with the spinors from numerical DFB calculations of the state averaged over the nonrelativistic  $4f^5 5d^1 6s^1 6p^1$  configuration (which differs from the generator state by the occupation number of the  $4f$  shell) of the Sm atom and the corresponding relative errors (in %) of their reproducing in calculations with different GRECP versions.

Spinor	DFB	Original	Original	Valence	Core	Core
	Fermi	GRECP	GRECP	GRECP	GRECP	GRECP
	(num.)	(num.)	(gauss.)			
					5spd, 4f	4spdf
	ME				Relative errors (in %)	
$4s_{1/2}$	0.377586	2.187	2.189	2.635	2.753	2.182
$4p_{1/2}$	0.400820	1.952	1.948	2.394	2.357	1.966
$4p_{3/2}$	0.437398	1.930	1.928	2.346	2.371	1.958
$4d_{3/2}$	0.510444	1.399	1.402	1.421	1.422	1.505
$4d_{5/2}$	0.525484	1.351	1.351	1.402	1.404	1.459
$4f_{5/2}$	0.991432	-0.057	-0.062	-0.938	-0.939	0.748
$4f_{7/2}$	1.01195	-0.055	-0.060	-0.919	-0.920	0.771
$5s_{1/2}$	2.23285	0.041	0.041	0.085	0.078	-0.901
$5p_{1/2}$	2.79755	0.021	0.021	0.056	0.059	-0.414
$5p_{3/2}$	3.10529	0.020	0.020	0.064	0.063	-0.408
$5d_{3/2}$	8.19197	-0.007	-0.006	-0.024	-0.038	0.564
$5d_{5/2}$	8.49997	-0.009	-0.009	-0.018	-0.032	0.501
$6s_{1/2}$	20.1753	-0.008	-0.008	0.039	0.120	2.597
$6p_{1/2}$	37.2712	-0.008	-0.009	0.018	-0.007	-4.082
$6p_{3/2}$	40.7918	-0.007	-0.007	0.022	0.000	-2.611